



7-Pyrrolidinethoxy-4'-Methoxyisoflavone Prevents Amyloid β -Induced Injury by Regulating Histamine H3 Receptor-Mediated cAMP/CREB and AKT/GSK3 β Pathways

Linlin Wang^{1,2†}, Jiansong Fang^{3†}, Hailun Jiang¹, Qian Wang¹, Situ Xue¹, Zhuorong Li^{1*} and Rui Liu^{1*}

OPEN ACCESS

Edited by:

Cesare Mancuso,
Università Cattolica del Sacro Cuore,
Italy

Reviewed by:

Damiana Leo,
University of Mons, Belgium
Domenica Donatella Li Puma,
Catholic University Medical School,
Italy

*Correspondence:

Zhuorong Li
lizhuorong@imb.pumc.edu.cn
Rui Liu
liurui@imb.pumc.edu.cn

† These authors have contributed
equally to this work

Specialty section:

This article was submitted to
Neuropharmacology,
a section of the journal
Frontiers in Neuroscience

Received: 19 December 2018

Accepted: 21 March 2019

Published: 10 April 2019

Citation:

Wang L, Fang J, Jiang H,
Wang Q, Xue S, Li Z and Liu R (2019)
7-Pyrrolidinethoxy-4'-
Methoxyisoflavone Prevents Amyloid
 β -Induced Injury by Regulating
Histamine H3 Receptor-Mediated
cAMP/CREB and AKT/GSK3 β
Pathways. *Front. Neurosci.* 13:334.
doi: 10.3389/fnins.2019.00334

¹ Institute of Medicinal Biotechnology, Chinese Academy of Medical Sciences & Peking Union Medical College, Beijing, China, ² Institute of Materia Medica, Chinese Academy of Medical Sciences & Peking Union Medical College, Beijing, China, ³ Institute of Clinical Pharmacology, Guangzhou University of Chinese Medicine, Guangzhou, China

In studies on the treatment of Alzheimer's disease (AD), in which cognition is enhanced even modestly or selectively, it has been considered that the histamine H3 receptor (H3R) may be a potential target. In this study, we aimed at evaluating the ability of 7-pyrrolidinethoxy-4'-methoxyisoflavone (indicated as LC1405), a novel potential H3R antagonist identified from our H3R antagonist screening system, to ameliorate amyloid β ($A\beta$)-induced cognitive deficits, and to explore the underlying mechanisms that are related to H3R-modulated signaling. Our results demonstrated that LC1405 effectively reduced the progression of $A\beta$ -associated disorders, such as improved learning and memory capabilities, preserved tissues from suffering neurodegeneration and ultrastructural abnormalities, and ameliorated cholinergic dysfunction in an APP/PS1 double transgenic mouse model of AD. In an *in vitro* model, LC1405 protected neuronal cells against copper-induced $A\beta$ toxicity, as demonstrated by the improvement in cell viability and decrease in neuronal apoptotic ratio. In addition, treatment with LC1405 resulted in the up-regulation of acetylcholine (ACh) or histamine release and provided neuroprotection through cellular signaling cascades involving H3R-mediated cAMP/CREB and AKT/GSK3 β pathways. Furthermore, the beneficial effects of LC1405 on $A\beta$ -mediated toxicity and H3R-mediated cAMP/CREB and AKT/GSK3 β axes were reversed after pharmacological activation of H3R. In conclusion, our results demonstrated that LC1405 blocked $A\beta$ -induced toxicity through H3R-modulated signaling transduction both *in vitro* and *in vivo*. The results also suggested that LC1405 might have translational potential as a complementary therapy to control disease progression in AD patients who developed cognitive deficits with H3R-related ACh neurotransmission abnormality.

Keywords: acetylcholine, Alzheimer's disease, amyloid beta-peptide, cyclic AMP response element binding protein, histamine H3 receptor

INTRODUCTION

Alzheimer's disease (AD), the most common cause of dementia in elderly population, is characterized by complicated and multifactorial pathophysiological alterations, primarily including senile plaque deposits, Tau protein hyperphosphorylation, high oxidative stress, metal ion dyshomeostasis, and neurotransmitter system irregularities (Ballard et al., 2011; Chiang and Koo, 2014). Currently, the principal treatment to combat AD in clinical practice involves the administration of acetylcholinesterase (AChE) inhibitors and the *N*-methyl-D-aspartate (NMDA) receptor antagonist memantine, which resulted in limited symptomatic improvement. However no effective treatment strategy is available that results in recovery or even retardation in the progression of the disease. Therefore, it is of utmost importance to develop novel and effective therapies for the treatment of AD.

Over the past decade, preclinical studies and clinical trials identified histamine H3 receptor (H3R), a histamine receptor subtype that is predominantly expressed in neurons of the central nervous system (CNS), as a possible target for cognition-enhancing candidates that may have beneficial effects on mild-to-moderate AD (Esbenshade et al., 2006; Bonaventure et al., 2007; Mani et al., 2017). Among the diverse H3R antagonists investigated up to now, two small H3R antagonists, ABT-239 and A-431404, showed procognitive effects in ketamine and MK-801-induced animal models (Brown et al., 2013). Pre-clinical studies demonstrated that several H3R antagonists ameliorate cognitive deficits and related behaviors in a substantial number of animal models characterized by learning or memory dysfunction (Browman et al., 2004).

In AD, H3R in the prefrontal cortex and hippocampus acts as a presynaptic auto-receptor coupled to G $\alpha_{i/o}$ -proteins that controls the synthesis and release of histamine, and as a heteroreceptor on histaminergic and non-histaminergic neurons in regulating the release of other neurotransmitters, including acetylcholine (ACh), dopamine, glutamate, norepinephrine, and gamma-aminobutyric acid (GABA) (Clapham and Kilpatrick, 1992; Ligneau et al., 1998; Bacciottini et al., 2002; Medhurst et al., 2007). Furthermore, within the neuronal intracellular signal transduction H3R participates in a variety of pathways (Clapham and Kilpatrick, 1992; Esbenshade et al., 2008; Bhowmik et al., 2014). When ligands bind to H3R-activated Gi proteins, adenylyl cyclase (AC) is inhibited, leading to decreased levels of cyclic adenosine monophosphate (cAMP) and reduced phosphorylation-activation of cAMP response element binding protein (CREB), a transcription factor that is closely related to cognitive functions (Bhowmik et al., 2014). In addition, pathological alterations of phosphatidylinositol-3-kinase/protein kinase B/glycogen synthase kinase 3 β (PI3K/AKT/GSK3 β) signaling transduction are due to β -amyloid (A β)-stimuli via a variety of signal transduction pathways, thereby amplifying A β -induced pathogenic responses in the brain through abnormal H3R agonistic reactions (Bhowmik et al., 2014). Accordingly, a large number of previous studies demonstrated that targeted activation of H3R in neurons resulted in an accelerated cognitive decline and aggravated A β -induced neuronal perturbation

in β -amyloid precursor protein (APP) transgenic mice, accompanied by progressive loss of cholinergic neurons and destructive signaling pathways involving cAMP/CREB and AKT/GSK3 β cascades (Bhowmik et al., 2014; Bardgett et al., 2011; Bitner et al., 2011). Therefore, the central role of H3R in AD suggests that it may be an attractive target in the development of novel therapies against diseases using H3R antagonists.

In the present study, we have investigated cognitive improvement and neuronal protection using a potential non-imidazole H3R antagonist, 7-pyrrolidinethoxy-4'-methoxyisoflavone (**Figure 1A**, indicated as LC1405) that has affinity with human H3R and high H3R inhibition power *in vitro*. We investigated its action against A β -induced neurotoxicity, and the underlying mechanisms of action against A β toxicity correlated with H3R-modulated signaling both in APP and presenilin 1 (PS1) double transgenic mice and copper-induced A β toxicity in APP Swedish mutation overexpressing SH-SY5Y cells.

MATERIALS AND METHODS

Animals and Drug Treatment

Heterozygous APP^{swe695}/PSEN1^{dE9} (APP/PS1) transgenic mice and age-matched wild-type (WT, C57BL/6) littermates were obtained from the Model Animal Research Center of Nanjing University (Nanjing, China). All animal studies were approved by the Institute of Medicinal Biotechnology, Chinese Academy of Medical Sciences (Beijing, China) and performed in accordance with ethical guidelines of the Experimental Animal Care and Use Committee.

Nine-month-old WT mice and APP/PS1 transgenic mice were randomly divided into four groups, including a WT control group ($n = 13$, seven males and six females), LC1405-treated WT group ($n = 13$, seven males and six females), APP/PS1 control group ($n = 13$, seven males and six females), and LC1405-treated APP/PS1 group ($n = 13$, seven males and six females). Mice in the WT+LC1405 and APP/PS1+LC1405 groups received an intragastric administration of LC1405 for 6 d/week at a dosage of 3 mg/kg. LC1405 was dissolved in 20% hydroxypropyl- β -cyclodextrin (CMC-Na), thus, mice in the control group received 20% CMC-Na according to the same modality. Drug treatment was performed for 20 weeks.

After behavioral tests, mice were divided into three groups for the parallel evaluation of different parameters. Three mice per group were transcardially perfused with normal saline solution, followed by 4% paraformaldehyde (PFA). Then, brains were collected and subjected to immunohistochemical staining and transmission electron microscopy. Four mice per group were chosen for the detection of oxidative stress, cholinergic activity, A β levels, and cAMP content in the brain. Four mice per group were prepared for quantification of H3R-mediated signaling transduction in the cortex and hippocampus, such as phosphorylated CREB, AKT, and GSK3 β using ELISA. The brain of the remaining mice was quickly removed and stored at -80°C until further experiments. The acetylcholine and histamine levels were evaluated in another two WT mouse groups

($n = 4$, two males and two females) that received an intragastric administration of LC1405 at a dosage of 3 mg/kg dissolved in CMC-Na or only CMC-Na as control. Mice were randomly selected for both the initial division into treatment groups and the subsequent selection for the three experiments.

Behavioral Assessment of Learning and Memory

Behavioral tests were performed when mice were thirteen months old, following 20 weeks of treatment with LC1405 or vehicle control. The Morris Water Maze (MWM) test is a classical visual-spatial learning technique used in rodents for assessing learning and memory capabilities hippocampus-dependent (Vorhees and Williams, 2006). Briefly, during the acquisition trial, mice were subjected to four training trials per day for five consecutive days. Both the escape latency (time required to find the platform) and swimming speed were recorded. At the end of the last trial, the platform was removed to proceed for the probe trial, which was carried out at 2 and 48 h post-training. The time the mice spent in the target quadrant and the frequency of passing through the platform were recorded.

Contextual short-term memory of the mice was assessed using a passive avoidance test (Nasehi et al., 2012). The apparatus consisted of illuminated (bright) and non-illuminated (dark) compartments. During the acquisition trial, mice were initially placed in the bright compartment for a maximum of 300 s, and upon entering the dark compartment received an electric foot shock (0.3 mA, 2 s). As a measure of memory retention, the initial latency of mice to enter the dark compartment and error times were recorded at 24 h after acquisition training.

Immunohistochemical Staining

The brain was embedded in paraffin and dissected into 8 μ M sections. Fluoro-Jade B (FJB, Histochem, Jefferson, AR, United States) and Thioflavin S (Thio S, Sigma, St. Louis, MO, United States) were used to evaluate neuronal degeneration and fibrillar A β level in hemi-brain tissue sections, respectively, and were performed using standard histological techniques as previously reported (Liu et al., 2014, 2018). Brain pathological features were evaluated on the sections under a fluorescence microscope (Olympus IX70, Olympus, Tokyo, Japan). The number of FJB-positive neurons and Thio S-positive neurons were manually evaluated as the number of neurons in 1 mm² of the cerebral cortex and hippocampus region. Cell count was obtained by averaging the counts from 10 sections per mouse.

Ultrastructural Analysis by Transmission Electron Microscopy

The prefrontal cortex and hippocampus were carefully harvested from the PFA-perfused brain of the experimental mice and placed overnight in the fixative [20 mL of 2.5% glutaraldehyde (Merck, Darmstadt, Germany) and 2.0% PFA (Beijing Chemical Works, Beijing, China) in 0.15 M cacodylate buffer (Merck, Darmstadt, Germany)]. Ultrathin sections were cut as previously described (Yu et al., 2015), and a LEO 906 transmission

electron microscope (Zeiss, Oberkochen, Germany) was used for ultrastructural imaging.

Measurement of Oxidative Stress and Cholinergic Activity in the Brain

The hemi-brains of APP/PS1 and WT mice were homogenized via ultrasonication, and centrifuged at 12,000 $\times g$ for 10 min at 4°C. The concentration of malondialdehyde (MDA), superoxide dismutase (SOD) and glutathione peroxidase (GSH-Px) within the homogenates was determined using commercial assay kits (Jiancheng Biotech, Nanjing, Jiangsu, China) in accordance with the corresponding manufacturer's instructions. ACh levels and the AChE activity were determined using the ultrasensitive Amplex@ red ACh/AChE assay kit (Molecular Probes, Paisley, United States) according to the manufacturer's guidelines.

Acetylcholine Quantification Using High-Performance Liquid Chromatography

For conventional analysis, brain tissue ACh levels were quantified using high-performance liquid chromatography (HPLC) coupled to electrochemical detection. In brief, ACh was separated on a BetaBasic C18 column (Thermo-Hypersil, Waltham, MA, United States; 150 mm \times 1.0 mm; particle size, 3 μ m) at a temperature of 25 °C using a mobile phase consisting of 100 mM Na₂HPO₄, 2.0 mM sodium octanesulfonic acid, 0.5 mM tetramethylammonium chloride and 100 μ L of Reagent MB microbicide (ESA Inc., Chelmsford, MA, United States), adjusting the pH to 8.0. The separated ACh fraction was placed in an enzyme reactor (Bioanalytical Systems) which yielded H₂O₂ for the detection with an enzyme-coated glassy carbon electrode with a potential set at 100 mV versus silver/silver chloride (Ag/AgCl). The sensitivity for ACh detection was approximately 0.5 fmol/15 μ L of sample. Chromatographic data were collected and quantified by comparison with known standard concentrations.

Histamine Determination Using High-Performance Liquid Chromatography

Brain histamine levels were determined by HPLC and quantified by fluorometric detection. Brains were homogenized in 3% perchloric acid solution containing 0.5 mM EDTA, and then centrifuged at 5500 $\times g$ for 15 min at 4°C. The supernatant was collected and histamine was separated using a Waters Atlantis C18 HPLC column (Milford, MA, United States; 150 mm \times 3.0 mm; particle size, 3 μ m) with a mobile phase containing 160 mM KH₂PO₄, 0.45 mM octanesulfonic acid, 1% methanol and 0.1 mM EDTA (pH 4.5), delivered at 0.5 to 0.7 mL/min. Using a T-piece, the eluent line was connected to the reagent line, through which a 0.02% solution of o-phthalaldehyde (OPA) was delivered in 0.15 M NaOH at a rate of 0.60 mL/min. The OPA reagent was mixed with the eluent in a mixing coil of metal tubing (outer diameter, 1.1 mm; inner diameter, 0.55 mm; length, 1 m) that enabled the derivatization

reaction at room temperature. The fluorescence of the reaction product was measured using a fluorometric detector (Ex/Em, 350 nm/450 nm). Chromatographic data were collected and quantified by comparison with known standard concentrations. The sensitivity for histamine detection was approximately 20 fmol/20 μ L of sample.

Cell Culture and Treatments

To evaluate the neuroprotective effects of LC1405, the Swedish mutant form of the human APP695 gene was stably transfected into SH-SY5Y cells that were purchased from the ATCC (ATCC[®]CRL-2266, Manassas, VA, United States), to establish an AD *in vitro* model (named APPsw cells). In this cell model, copper acts as a promotor for triggering A β -mediated neurotoxicity when added as a stimulator into the culture medium (Zhang et al., 2006; Zhao et al., 2013). Cells were cultured in DMEM/F12 medium (Invitrogen, Carlsbad, CA, United States) supplemented with 10% fetal calf serum (Invitrogen, Carlsbad, CA, United States) and incubated at 37°C in a humidified chamber containing 5% CO₂. The detailed protocol and groups were as follows. Cells were randomly divided into two groups: one group was supplemented with 300 μ M copper, whereas the other was not (indicated as control cells). The group supplemented with copper was divided into subgroups based on LC1405 concentrations as follows: 0 μ M (copper-treated APPsw cells), 0.03 μ M, 0.1 μ M, 0.3 μ M, 1.0 μ M, 3.0 μ M, and 10.0 μ M. Different concentrations of LC1405 were added at the start of copper-initiated injury, then cells were incubated for 24 h at 37°C. To determine whether H3R inhibition was involved in the neuroprotective effects of LC1405 against A β toxicity, the specific agonists of H1 to H4, 2-(3-trifluoromethylphenyl) histamine (FMPH), amthamine dihydrobromide, (R)-(α)-(-)-methylhistamine dihydrobromide (RAMH) and VUF-8430 were used. Cells were pretreated with the specific agonists at 1.0 μ M for 30 min at 37°C before being treated with LC1405.

Cell Viability Assay

Viability was determined by 3-(4,5-dimethylthiazol-2-yl)-5-(3-carboxymethoxyphenyl)-2-(4-sulfophenyl)-2H-tetrazolium (MTS, Promega, Madison, WI, United States). In brief, cells were incubated for 4 h at 37°C with an appropriate amount of MTS according to the manufacturer's instructions. The soluble product formazan was detected using a Spark 20M multimode microplate reader (Tecan Group Ltd., Mannedorf, Switzerland) at 490 nm.

Cell Immunofluorescence Assay

Cell immunofluorescence is a sensitive fluorescence-based multiparametric technology that is used to determine the expression and activity of proteins within a cell. Cells were seeded in a 96-well plate at a density of 8000 cells/well in 200 μ L medium/well and subjected to all treatments described in the section 2.8. The apoptotic ratio *in vitro* was determined by simultaneous staining with acridine orange (AO) and ethidium bromide (EB) (Sigma-Aldrich, St. Louis, MO, United States). After treatment with LC1405 at different

concentrations, 100 μ g/mL AO and 100 μ g/mL EB were added to the cells and incubated for 15 min at 37°C. The expression of β -APP, p-CREB, and p-PI3K was quantified using cell immunofluorescence routine procedures as previously described (Liu et al., 2012). The following primary polyclonal rabbit antibodies were used: anti- β -APP [1:500, Cell Signaling Technology (CST), Danvers, MA, United States], anti-p-CREB (Ser133) (1:120, CST), and anti-p-PI3K p85 α (Y607) (1:80, Abcam, Cambridge, MA, United States). The fluorescent secondary antibodies used were goat anti-rabbit conjugated with Alexa Fluor 488 or Alexa Fluor 546 (1:1000, Invitrogen, Carlsbad, CA, United States). The apoptotic ratio and mean fluorescence intensity were determined and analyzed using a Cellomics ArrayScan^{VTI} HCS Reader (Cellomics Inc., Pittsburgh, PA, United States) running Morphology Explorer BioApplication software for the average of 20 fields of view in each selected well.

Determination of A β and cAMP Concentrations

After the treatment, mouse hemi-brains and APPsw cells were separately homogenized using ultrasonication and centrifuged at 12,000 \times g for 10 min at 4°C. An aliquot of mouse hemi-brains or APPsw cells after homogenization was resuspended in 2% sodium dodecyl sulfate (SDS) containing protease inhibitors. After centrifugation, the supernatant was collected for the detection of soluble A β . The remaining SDS-insoluble pellet was sonicated, dissolved in 70% formic acid, and centrifuged for 60 min at 100,000 \times g, and the supernatant was collected for the detection of insoluble A β . The concentration of both soluble and insoluble A β was quantified using commercially available ELISA kits (BioSource, Camarillo, CA, United States) specific for the detection of human A β _{1–40/42}. In addition, soluble A β oligomers (oA β) were detected using western blot as previously described (Liu et al., 2018). Another aliquot of mouse hemi-brains was homogenized in RIPA buffer (Cell Signaling Technology, Danvers, MA, United States) containing protease inhibitor, phosphatase inhibitor, and phenylmethyl sulfonyl fluoride (PMSF). Forty μ g protein per lane were run on polyacrylamide gel, transferred onto a polyvinylidenedifluoride membrane, blocked with 5% BSA in Tris-buffer saline containing 0.1% Tween-20 (TBST) for 2 h, and subsequently incubated with the primary antibody overnight, using the rabbit anti-oligomer conformation-specific A11 (pre-fibrillar A β oligomer, 1:1000, Invitrogen, Carlsbad, CA, United States) diluted in blocking solution. Membranes were washed with TBST prior to incubation with horseradish peroxidase-labeled (HRP)-linked secondary antibody (1:1000, ZSGB-Bio, Beijing, China) at room temperature for 1 h. The signals were detected using an enhanced chemiluminescence kit. Chemiluminescence image acquisition and densitometric band quantitation were performed using Fusion-FX6 imaging system (Vilber Lourmat, Marne-la-Valle, France). The cAMP concentration was determined using a cAMP assay kit (R&D Systems, Minneapolis, MN, United States) in accordance with the manufacturer's guidelines.

Quantification of Phosphorylated CREB, AKT, and GSK3 β Using ELISA

After the treatment, the cortex and hippocampal tissue of APP/PS1 and WT mice and APPsw cells were homogenized after addition of RIPA buffer (CST, Danvers, MA, United States) containing protease inhibitors, phosphatase inhibitors, and PMSE, then centrifuged at $20,000 \times g$ for 15 min at 4°C. The protein concentration of the samples was quantified using a commercially available bicinchoninic acid (BCA) kit (Thermo Fisher Scientific, Rockford, IL, United States). ELISA kits were used for quantification of phospho-CREB (Ser133, R&D Systems, Minneapolis, MN, United States), phospho-AKT (Ser473, R&D Systems) and phospho-GSK3 β (Ser9, CST, Danvers, MA, United States) activity in accordance with the manufacturers' guidelines.

In vitro BACE-1 Assay

The ability of LC1405 at concentrations ranging from 0.3 and 300.0 μ M to inhibit beta-site APP-cleaving enzyme (BACE-1) activity was determined using a BACE-1 assay kit according to the manufacturer's guidelines.

Statistical Analysis

Data were analyzed using SPSS software (version 18.0, SPSS, Inc., Chicago, IL, United States), and presented as mean \pm standard error of the mean (SEM). Statistical analysis was performed by using different tests as follows: (1) escape latency of the MWM test the acquisition trial was analyzed using the ANOVA for repeated measures (training days and treatment, with treatment as main effect), and one-way ANOVA with Tukey's *post hoc* analyses were used to analyze treatment differences (treatment as main effect); (2) treatment differences in the probe trials, pathological and biochemical assays, and *in vitro* studies were performed using a one-way ANOVA, followed by Tukey's *post hoc* testing to analyze the differences between groups; (3) the area under the curve (AUC) of histamine and ACh levels in the brain after LC1405 administration were analyzed by student *t*-test. The statistical significance was set at a *p*-value of less than 0.05.

RESULTS

LC1405 Treatment Improves Cognitive Deficits in APP/PS1 Mice

At 13 months of age, APP/PS1 mice underwent behavioral testing using the MWM test, a widely-accepted test for spatial learning and memory capability. During the acquisition trial, the escape latency to the target platform for all mice is illustrated in **Figure 1B**. Significant differences on escape latency within groups [$F_{(4,192)} = 138.697, p < 0.001$] and a significant treatment effect on escape latency were found [$F_{(3,48)} = 20.572, p < 0.001$]. Subsequent *post hoc* comparison illustrated that treatment with 3 mg/kg of LC1405 was considerable in improving the spatial learning ability in APP/PS1 mice compared to APP/PS1 control mice ($p < 0.05$). Probe trials were carried out to evaluate short-term memory at 2 h and long-term memory at 48 h following

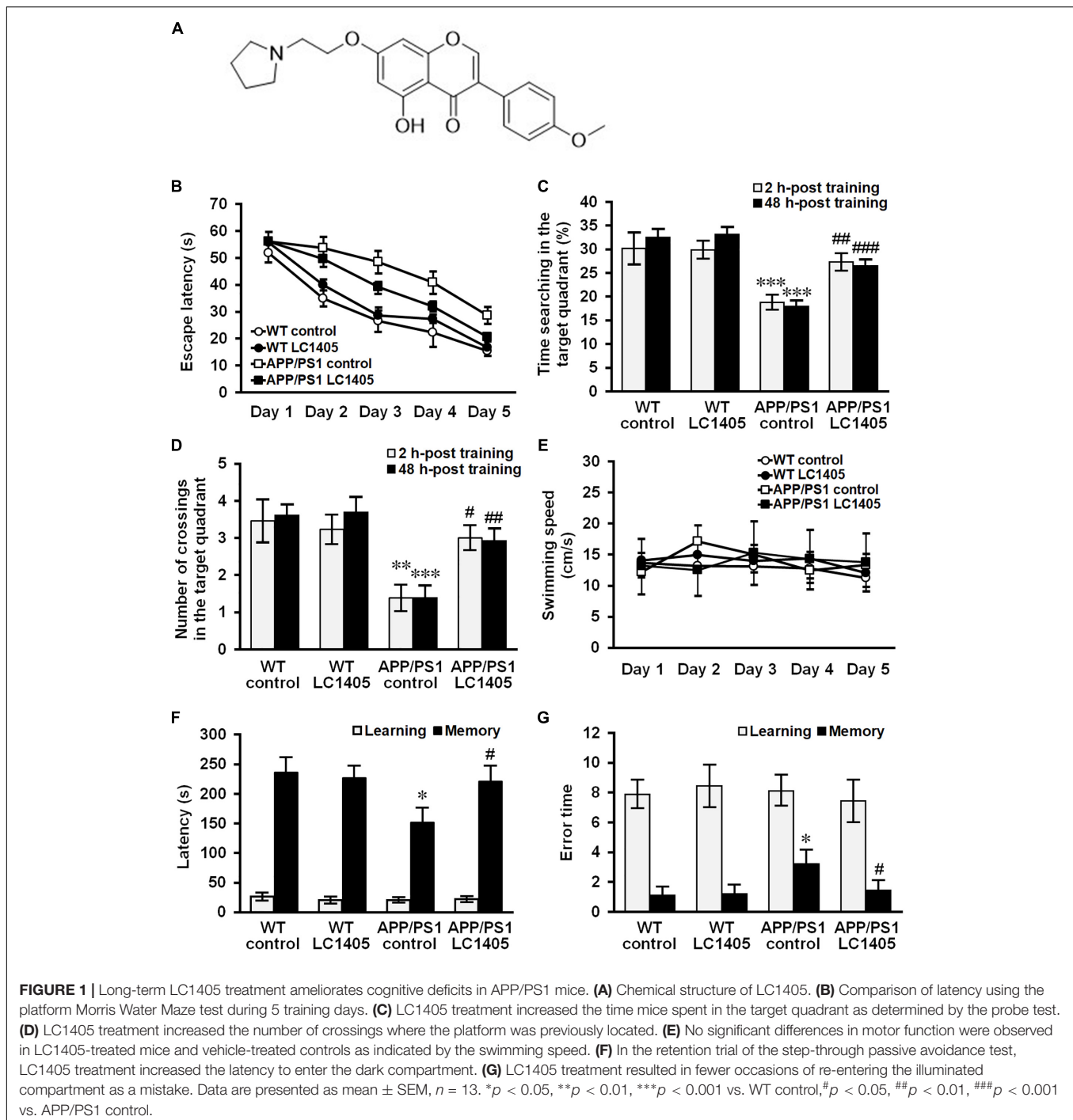
the five-consecutive-day trials. Our data indicated that APP/PS1 control mice stayed for a shorter time and completed fewer crossings in the target quadrant at both time points compared with WT control mice (**Figures 1C,D**) (2 h: $18.77 \pm 1.25\%$ vs. $30.14 \pm 3.04\%$, 1.38 ± 0.31 vs. 3.46 ± 0.52 , $p < 0.001$ and 0.01 ; 48 h: $17.94 \pm 0.85\%$ vs. $32.51 \pm 1.37\%$, 1.38 ± 0.29 vs. 3.62 ± 0.24 , both $p < 0.001$), while LC1405-treated APP/PS1 mice stayed in the target quadrant for a longer time (2 h: $27.29 \pm 1.47\%$ vs. $18.77 \pm 1.25\%$, $p < 0.01$; 48 h: $26.51 \pm 0.87\%$ vs. $17.94 \pm 0.85\%$, $p < 0.001$), and performed more crossings at the platform location compared with APP/PS1 control mice (2 h: 3.00 ± 0.29 vs. 1.38 ± 0.31 , $p < 0.05$; 48 h: 2.92 ± 0.28 vs. 1.38 ± 0.29 , $p < 0.01$). Moreover, our results demonstrated no significant differences in swimming speed among treatment groups in the acquisition trial (**Figure 1E**), suggesting that the improvement on learning capability in LC1405-treated APP/PS1 mice was not due to locomotor ability.

During the retention trial in the passive avoidance test, APP/PS1 control mice re-entered the illuminated compartment more frequently with shorter step-through latency compared to WT control mice (**Figures 1F,G**) (151.58 ± 24.22 s vs. 236.57 ± 24.14 s, 3.22 ± 0.82 vs. 1.11 ± 0.45 , both $p < 0.05$), while LC1405-treated APP/PS1 mice showed less tendency toward the illuminated compartment, involving longer step-through latency and fewer numbers of errors compared to APP/PS1 control mice (220.75 ± 26.25 s vs. 151.58 ± 24.22 s, 1.44 ± 0.58 vs. 3.22 ± 0.82 , both $p < 0.05$), indicating that LC1405 treatment ameliorated memory dysfunction.

In WT mice, LC1405 treatment did not affect cognitive capabilities in the behavioral tests performed, therefore we concluded that long-term oral administration of LC1405 plays a role in ameliorating A β -dependent cognitive deficits rather than affecting functions that are normal.

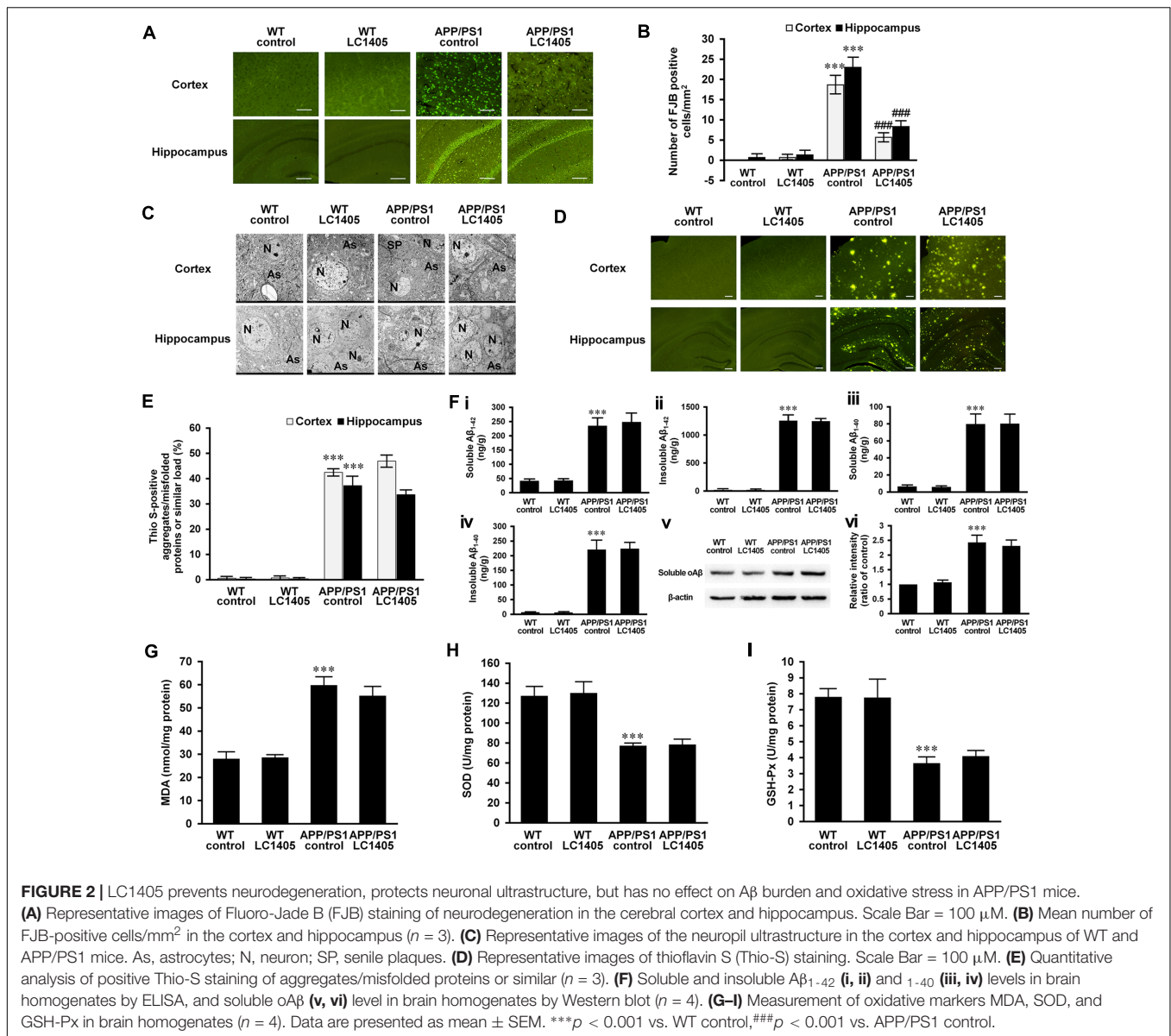
LC1405 Prevents Neuronal Degeneration and Protects Ultrastructure, but Has No Substantial Effect on the Reduction of A β Burden or Oxidative Markers in APP/PS1 Mice

FJB is a useful marker for the identification of neuronal degeneration because of its ability to stain the entire neuron, such as the cell body, dendrites, axons, and axon terminals (Ballok et al., 2003). In both the cerebral cortex and the hippocampus of WT control and LC1405-treated WT mice, FJB-positive neurons were rarely detected. However, in the cortical and hippocampal regions of APP/PS1 mice, the number of FJB-positive neurons was significantly increased (**Figures 2A,B**) (cortex: 18.67 ± 2.02 vs. 0; hippocampus: 23.00 ± 2.30 vs. 0.67 ± 0.67 ; both $p < 0.001$) compared to WT control mice. LC1405 treatment decreased the number of FJB-positive neurons in the cortex and hippocampus of APP/PS1 mouse brains compared to APP/PS1 control group (cortex: 5.67 ± 0.88 vs. 18.67 ± 2.02 ; hippocampus: 8.33 ± 1.20 vs. 23.00 ± 2.30 ; both $p < 0.001$), indicating that LC1405 treatment relieved the degenerative pathology in APP/PS1 mouse brain.



To further evaluate degenerative changes at the ultrastructural level, sections of the cortex and hippocampus were observed using a transmission electron microscope (Figure 2C). The cortical and hippocampal regions of WT control and LC1405-treated WT mice were well-characterized, showing a compact neuropil appearance with normal neurons (N) and astrocytes (As), with no swelling or shrinkage. In APP/PS1 mouse brain regions, neuropils were disrupted and neuronal degeneration was detected as the neurons showed a shrunken appearance.

Degenerative neurons were embodied in the ruptured neuronal membranes, with cytoplasm containing dark granules, and condensed nuclei. In addition to degeneration of adjacent neuropils, intracellular vacuolation and astrocyte edema were observed, accompanied with A β plaques (SP) deposited in the neuropils nearby. LC1405 treatment attenuated neuropil degeneration in the cortex and hippocampus of LC1405-treated APP/PS1 mice. Signs of swelling and disintegration of astrocytes were disappeared, and A β plaque deposition was less apparent



in surrounding neuropils. Together, these findings indicated that LC1405 treatment was effective in preventing A β -mediated neuronal degeneration.

Overproduction and aggregation of A β are considered key pathological events in the neurodegenerative cascade in AD. Although in this study neuronal degeneration and neuropil ultrastructure were ameliorated by LC1405 treatment, A β aggregates/misfolded proteins or similar in the cortex and hippocampus as indicated by Thio S staining, were not reduced after long-term oral administration of LC1405 (**Figures 2D,E**) (cortex: 46.93 ± 1.98 vs. 42.27 ± 1.71 ; hippocampus: 33.67 ± 1.43 vs. 37.23 ± 3.32). Similarly, the levels of soluble or insoluble A β_{1-42} or A β_{1-40} in the brain did not significantly decrease following LC1405 treatment (**Figures 2Fi–iv**) (soluble A β_{1-42} : 246.80 ± 28.48 ng/g vs. 233.47 ± 25.05 ng/g; insoluble A β_{1-42} : 1236.65 ± 34.57 ng/g vs. 1246.66 ± 87.17 ng/g;

soluble A β_{1-40} : 79.57 ± 10.45 ng/g vs. 79.18 ± 11.08 ng/g; insoluble A β_{1-40} : 221.98 ± 20.29 ng/g vs. 218.87 ± 31.29 ng/g). Furthermore, the increased level of A11-immunoreactive prefibrillar oligomers, which represented the presence of potential neurotoxic A β oligomers and then underwent a concerted conformation change from protofibrils to form fibrils (Glabe, 2008; Gulisano et al., 2018), could not be significantly decreased by LC1405 treatment either (**Figures 2Fv,vi**) (ratio of WT control: 2.31 ± 0.20 vs. 2.43 ± 0.25). Combined, these data suggested that LC1405 treatment did not have a substantial effect in reducing A β levels in APP/PS1 mouse brain.

Oxidative stress is implicated in the pathology of AD, and in this study, the APP/PS1 mouse model displayed alterations in markers of oxidative stress in the brain, such as MDA, SOD, and GSH-Px compared to WT control group (**Figures 2G–I**) (MDA: 59.63 ± 3.32 nmol/mg protein vs. 27.87 ± 2.69 nmol/mg

protein; SOD: 76.33 ± 2.25 U/mg protein vs. 126.78 ± 8.72 U/mg protein; GSH-Px: 3.62 ± 0.35 U/mg protein vs. 7.78 ± 0.47 U/mg protein; all $p < 0.001$). However, these markers were not significantly ameliorated in APP/PS1 mouse brain after treatment with LC1405 (MDA: 55.03 ± 3.71 nmol/mg protein vs. 59.63 ± 3.32 nmol/mg protein; SOD: 78.72 ± 6.10 U/mg protein vs. 76.33 ± 2.25 U/mg protein; GSH-Px: 4.06 ± 0.31 U/mg protein vs. 3.62 ± 0.35 U/mg protein).

LC1405 Treatment Does Not Alter AChE Activity in APP/PS1 Mouse Brain Tissue, but Increases the Level of ACh and Improves the Release of Histamine and ACh

Due to an early and severe depletion of cholinergic innervations in AD pathology, a decrease in AChE activity in the brain is a consistent finding (Dumas and Newhouse, 2011; Carvajal et al., 2013). A slight decrease in AChE activity was observed in APP/PS1 mouse brain, and LC1405 treatment did not alter the AChE activity significantly either in APP/PS1 or in WT mouse brain (Figure 3A) (LC1405-treated WT vs. WT control: 1.05 ± 0.10 vs. 1.00 ± 0.06 ; LC1405-treated APP/PS1 vs. APP/PS1 control: 0.79 ± 0.11 vs. 0.84 ± 0.08). Up-regulated ACh levels were observed in LC1405-treated WT and APP/PS1 mice compared to the correspondent LC1405-untreated groups (Figure 3B) (LC1405-treated WT vs. WT control: 2285.69 ± 123.96 pg/g vs. 1900.43 ± 82.70 pg/g, $p < 0.05$; LC1405-treated APP/PS1 vs. APP/PS1 control: 1761.88 ± 59.18 pg/g vs. 1222.23 ± 62.42 pg/g, $p < 0.01$), suggesting that LC1405 might be effective in increasing the responsiveness of ACh in cholinergic neurons.

In subsequent studies, the concentration of histamine and ACh were compared in the brain of WT mice with and without LC1405 treatment. After LC1405 administration, changes in ACh and histamine levels were expressed in terms of the area under the

curve (AUC) for a 0 to 4 h time-period. The time course results of histamine following LC1405 treatment revealed its rapid release that peaked within 30–60 min of dosing and persisted over the 4 h test period. In addition, ACh levels increased over the 60-min period after administration. When comparing the responses with the results of WT control mice, significant increases in AUC in histamine and ACh levels were observed after administration of 3 mg/kg LC1405 (Figures 3C,D) (histamine: 14.61 ± 2.05 vs. 3.72 ± 0.72 , $p < 0.001$; ACh: 20.27 ± 5.64 vs. 2.64 ± 0.80 , $p < 0.05$). This was not only the maximal response of ACh after LC1405 treatment, but a sustained increase in the brain after treatment from 60 to 120 min. The response of ACh could be a consequence of increased histamine release. Therefore, these results suggested that LC1405 might act on H3R, thereby leading to an overall increase in histamine and ACh levels.

LC1405 Treatment Modifies H3R-Mediated Signaling in APP/PS1 Mouse Brain

To identify whether H3R inhibition was a result of the treatment with LC1405, the downstream signaling pathways of H3R coupling were evaluated to assess the potential therapeutic efficacy. Our results showed that transduction of the cAMP/CREB pathway changed significantly in the brains of APP/PS1 mice, which showed a significant decrease in cAMP and p-CREB levels, of 76.12 and 62.78%, respectively in 13-month-old APP/PS1 mice when compared with the WT control (Figures 3E,F, all $p < 0.001$). The Tukey's *post hoc* comparison demonstrated that oral administration of LC1405 resulted in increased cAMP levels and upregulated p-CREB activity in APP/PS1 mouse brain compared to APP/PS1 control group (cAMP: 1.55 ± 0.17 nmol/mg protein vs. 0.66 ± 0.06 nmol/mg protein; p-CREB: 1.41 ± 0.14 ng/mg protein vs. 0.72 ± 0.09 ng/mg protein, 1.68 ± 0.11 ng/mg protein vs. 0.76 ± 0.09 ng/mg protein; all $p < 0.001$).

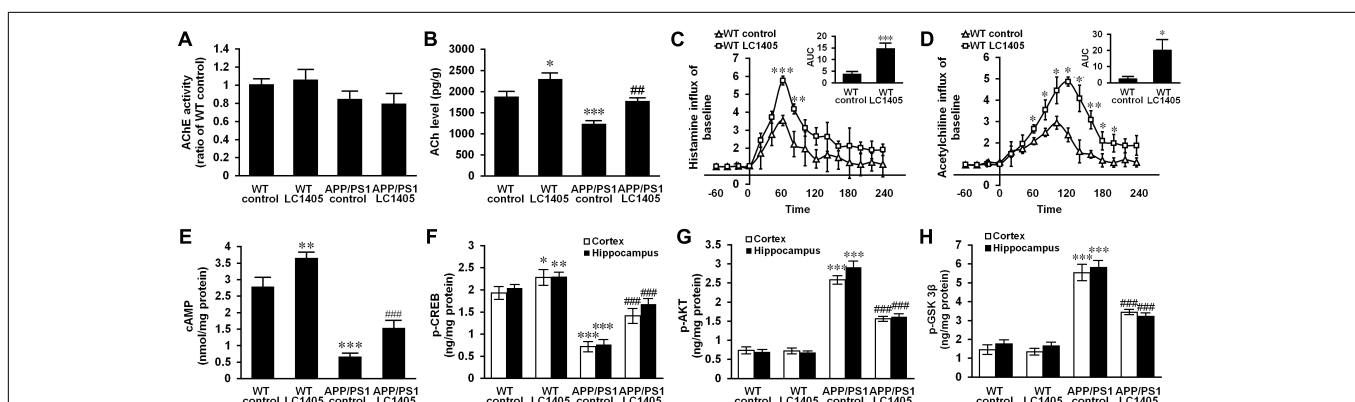


FIGURE 3 | LC1405 treatment increases the level of ACh and histamine and modifies H3R-mediated signaling in APP/PS1 mouse brain. **(A)** LC1405 treatment did not alter AChE activity in mouse brain ($n = 4$). **(B)** LC1405 treatment increased ACh level in the brain of WT and APP/PS1 mice ($n = 4$). **(C,D)** LC1405 treatment stimulated histamine and ACh responses in WT mouse brain ($n = 4$). **(E)** LC1405 treatment increased cAMP levels in WT and in APP/PS1 mouse brain ($n = 4$). **(F)** LC1405 treatment up-regulated p-CREB level in the cerebral cortex and hippocampus of WT and APP/PS1 mice ($n = 4$). **(G,H)** LC1405 treatment increased the signaling transduction of AKT/GSK3 β in the cerebral cortex and hippocampus of APP/PS1 mice ($n = 4$). Data are presented as mean \pm SEM. * $p < 0.05$, ** $p < 0.01$, *** $p < 0.001$ vs. WT control, ## $p < 0.01$, ### $p < 0.001$ vs. APP/PS1 control.

It should be noted that LC1405 treatment also activated cAMP/CREB cascades in WT control mice, indicating that an oral dose of 3 mg/kg of LC1405 affected basal transduction in normal brain (cAMP: 3.66 ± 0.13 nmol/mg protein vs. 2.79 ± 0.25 nmol/mg protein; p-CREB: 2.28 ± 0.15 ng/mg protein vs. 1.93 ± 0.12 ng/mg protein, 2.29 ± 0.08 ng/mg protein vs. 2.04 ± 0.07 ng/mg protein; $p < 0.05-0.01$). Thus, cAMP/CREB pathway transduction following H3R inhibition might play a role in the action of LC1405.

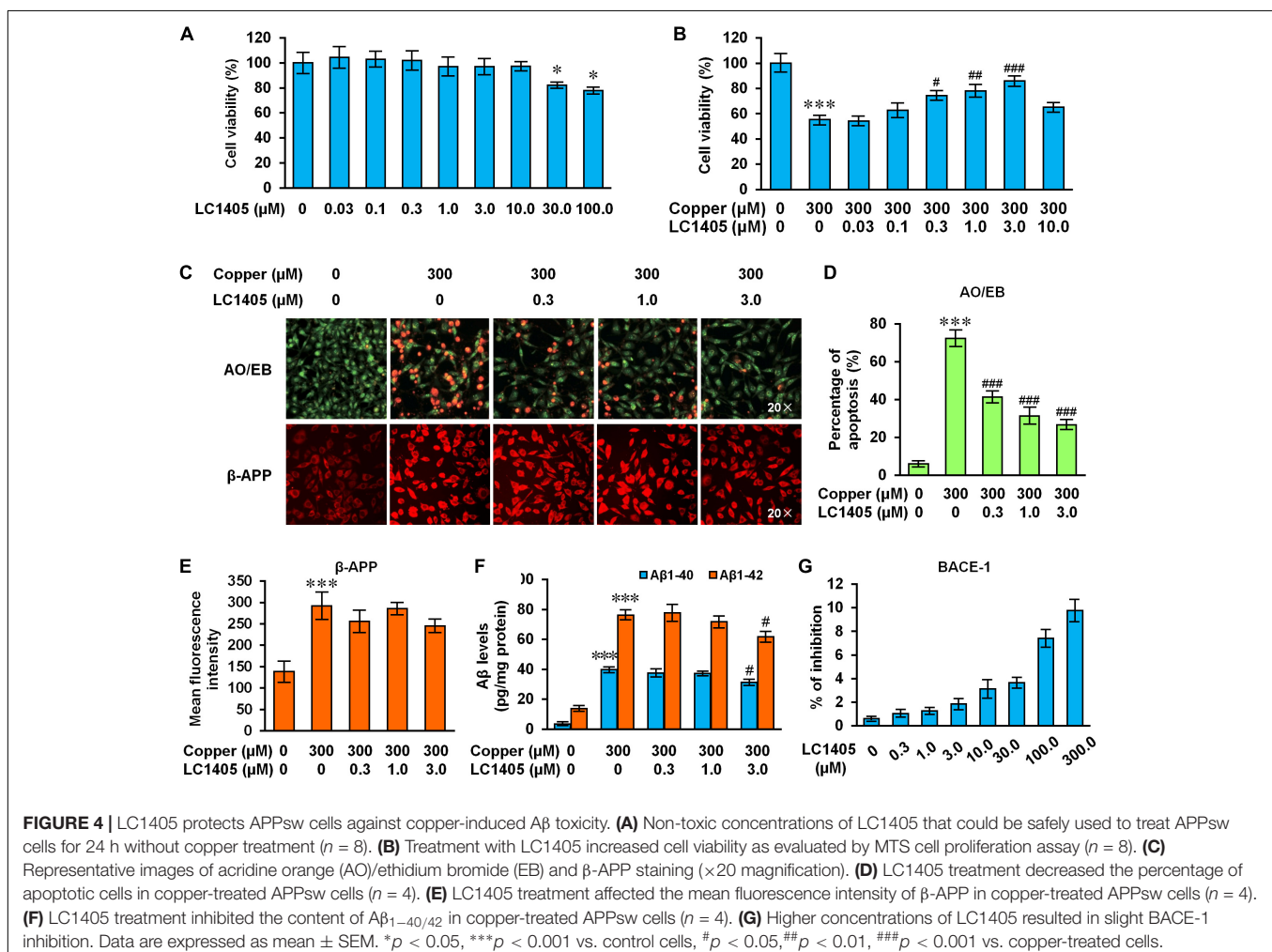
To investigate H3R downstream signaling, modification of the AKT/GSK3 β axis was evaluated. Up-regulation of phosphorylated AKT was accompanied by a high level of GSK3 β phosphorylation in the cortex and hippocampus of APP/PS1 mice compared to WT control group (Figures 3G,H) (p-AKT: 2.58 ± 0.09 ng/mg protein vs. 0.73 ± 0.06 ng/mg protein, 2.91 ± 0.15 ng/mg protein vs. 0.69 ± 0.04 ng/mg protein; p-GSK3 β : 5.54 ± 0.40 ng/mg protein vs. 1.45 ± 0.20 ng/mg protein, 5.82 ± 0.31 ng/mg protein vs. 1.76 ± 0.15 ng/mg protein; all $p < 0.001$). However, LC1405 treatment suppressed the phosphorylation in APP/PS1 mice (p-AKT: 1.56 ± 0.04 ng/mg protein vs. 2.58 ± 0.09 ng/mg protein, 1.61 ± 0.05 ng/mg protein vs. 2.91 ± 0.15 ng/mg protein; p-GSK3 β : 3.44 ± 0.09 ng/mg

protein vs. 5.54 ± 0.40 ng/mg protein, 3.22 ± 0.11 ng/mg protein vs. 5.82 ± 0.31 ng/mg protein; all $p < 0.001$), suggesting that LC1405 might be able to reverse the activated signaling of AKT/GSK3 β in AD.

LC1405 Protects Neuronal Cells Against Copper-Induced A β Toxicity *in vitro*

To better mimic Alzheimer's deficits, copper treatment was used to study metal ion imbalance triggering A β neurotoxicity using cells overexpressing the Swedish mutant form of human APP (Zhang et al., 2006; Liu et al., 2012). Before evaluating the protective effects of LC1405, we first established its safe, non-toxic dose in APPsw cells without copper treatment. Our results indicated that LC1405 concentration ranging between 0.03 and 10.0 μ M over 24 h did not have any toxic effect (Figure 4A). However, in the presence of 300 μ M copper, LC1405 significantly increased cell viability at 0.3 μ M, 1.0 μ M, and 3.0 μ M in a concentration-dependent manner (Figure 4B) ($74.46 \pm 2.99\%$, $78.15 \pm 4.12\%$, $85.93 \pm 3.40\%$ vs. $55.30 \pm 3.22\%$, $p < 0.05-0.001$).

Similar findings were observed in cells stained with the AO/EB apoptosis-detection dye. The normal morphology of control cells



was characterized by the presence of green-colored nuclei and an intact structure, whereas apoptotic characteristics included shrinkage, membrane blebbing, chromatin condensation, and the formation of apoptotic bodies were found in copper-treated APPsw cells. In the presence of copper, the proportion of APPsw cells undergoing apoptosis was $72.43 \pm 3.76\%$ compared to control cells (Figures 4C,D, $p < 0.001$). LC1405 treatment at concentrations of $0.3 \mu\text{M}$, $1.0 \mu\text{M}$, and $3.0 \mu\text{M}$ rescued the morphological changes indicative of apoptosis, and reduced the percentage of cells positively stained for the apoptosis-detection dye in a concentration-dependent manner compared with the cells treated with copper ($41.41 \pm 2.55\%$, $31.42 \pm 3.78\%$, $26.77 \pm 1.92\%$ vs. $72.43 \pm 3.76\%$, all $p < 0.001$). Combined with these protective effects, LC1405 concentrations at $0.3 \mu\text{M}$, $1.0 \mu\text{M}$, and $3.0 \mu\text{M}$ were chosen to investigate the underlying mechanism of LC1405 protection in the AD *in vitro* model.

LC1405 Has Limited Effects on Decreasing β -APP Expression or Attenuating A $\beta_{1-40/42}$ Levels

A β peptides are primarily generated from the cleavage of APP, which represent the major pathological event in the development of AD. In the present study, administration of copper increased the expression of β -APP by 2.11 fold. Similarly, the levels of A β_{1-40} and A β_{1-42} in APPsw cells increased respectively by 11.65 and 5.56 fold (Figures 4C,E,F, all $p < 0.001$). Treatment with LC1405 at the tested concentrations did not significantly reduce the expression of β -APP or the levels of A β_{1-40} and A β_{1-42} in APPsw cells, except at the highest concentration of $3.0 \mu\text{M}$ that showed an effect on inhibiting A $\beta_{1-40/42}$ levels by the reduction of 21.35% and 23.15% (Figure 4F, both $p < 0.05$). Moreover, LC1405 at higher concentrations (100 and $300 \mu\text{M}$) resulted in a slight BACE-1 inhibition (Figure 4G, $7.42 \pm 0.64\%$ and $9.76 \pm 0.83\%$), what was outside the range of concentrations tested in AD cells. Thus, our results suggested that LC1405 treatment might be independent of A β overproduction in the β -amyloidogenic pathway.

H3R Inhibition Contributes to the Neuroprotective Effects of LC1405 Against A β -Induced Toxicity

LC1405 might be identified as a candidate H3R antagonist with neuroprotection through virtual screening, serial cell-based assays, and extensive neuroprotection evaluation. In view of the Bayesian prediction, LC1405, as a potential H3R ligand, serves as a reference compound (Supplementary Table 2). In target functional activity assays *in vitro*, LC1405 showed substantial antagonistic effects combined with a relative high affinity for human and rat H3R, but relatively lower affinities for H1, H2, and H4 subtypes (Supplementary Table 2). Furthermore, LC1405 itself blocked the decrease of cAMP induced by RAMH (Supplementary Table 2), indicating that LC1405 might interact with H3R, thereby directly increasing cAMP levels. Importantly, LC1405 treatment exerted neuroprotective effects on rat primary cortical neurons against A β_{25-35} - and fibrillar A β_{1-40} (fA β_{1-40})-induced toxicity at $0.3 \mu\text{M}$, $1.0 \mu\text{M}$, and

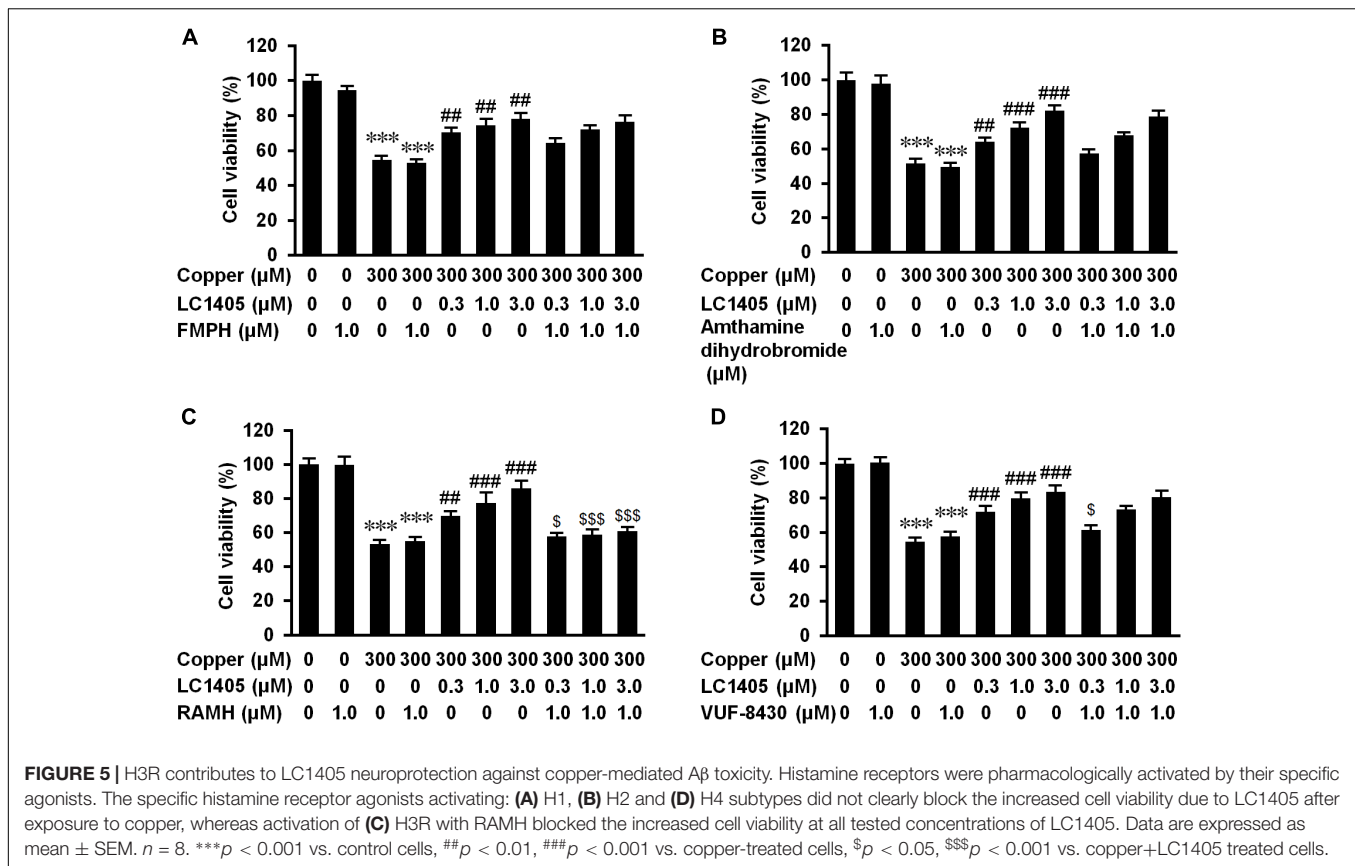
$3.0 \mu\text{M}$ in a concentration-dependent manner (Supplementary Figure 2, $p < 0.05-0.001$).

To determine whether H3R contributed to LC1405-mediated neuroprotection against A β -induced cytotoxicity, specific H3R agonist and other histamine receptor subtype agonists were used. As shown in Figure 5C, pharmacological activation of H3R with RAMH blocked the ability of LC1405 to rescue the decreased cell viability observed after exposure to copper at all the tested concentrations ($57.84 \pm 1.07\%$ vs. $69.80 \pm 1.56\%$, $58.96 \pm 1.63\%$ vs. $77.44 \pm 5.07\%$, $60.91 \pm 1.15\%$ vs. $86.01 \pm 3.27\%$, $p < 0.05-0.001$). Other specific histamine receptor agonists that activated H1, H2, and H4 subtypes did not exert any substantial effect (Figures 5A,B) or only partly reduced cell viability that had been increased by LC1405 (Figure 5D, $61.40 \pm 1.66\%$ vs. $71.87 \pm 2.13\%$, $p < 0.05$: copper-injured APPsw cells treated with LC1405 and VUF-8430 vs. copper-injured APPsw cells treated with LC1405). Thus, these results suggested that neuroprotection due to LC1405 against copper-induced A β injury might be largely attributable to its inhibitory effects on H3R.

H3R Mediates the Neuroprotective Effect of LC1405 Against A β Injury Through cAMP/CREB and PI3K/AKT/GSK3 β Signaling Pathways

Histamine H3 receptor signaling caused negative coupling of AC, thereby decreasing the intracellular activity of the cAMP/PKA pathway, subsequently reducing CREB levels (Bhowmik et al., 2014). In APPsw cells subjected to copper, a significant reduction in the intracellular of cAMP level and a significant decrease in phosphorylated CREB level were observed compared to the ones without copper treatment (Figures 6A–C) (cAMP: 64.04 ± 2.06 nmol/mg protein vs. 84.92 ± 2.51 nmol/mg protein; p-CREB: 182.82 ± 7.39 vs. 772.98 ± 19.03 ; both $p < 0.001$), indicating that the cAMP/CREB signaling pathway was inhibited in response to copper-triggered A β toxicity. LC1405 treatment contrasted A β -neurotoxicity by increasing intracellular levels of cAMP and up-regulating phosphorylated CREB, both in a concentration-dependent manner (cAMP: 76.27 ± 0.91 nmol/mg protein, 79.97 ± 0.84 nmol/mg protein, 81.71 ± 2.61 nmol/mg protein vs. 64.04 ± 2.06 nmol/mg protein; p-CREB: 280.07 ± 9.85 , 302.98 ± 11.49 , 359.74 ± 16.54 vs. 182.82 ± 7.39 ; $p < 0.05-0.001$). However, these effects of LC1405 were abolished at all the tested concentrations by the pharmacological activation of H3R treated with RAMH (cAMP: 63.48 ± 2.88 nmol/mg protein vs. 76.27 ± 0.91 nmol/mg protein, 64.10 ± 2.95 nmol/mg protein vs. 79.97 ± 0.84 nmol/mg protein, 65.92 ± 4.11 nmol/mg protein vs. 81.71 ± 2.61 nmol/mg protein; p-CREB: 202.51 ± 6.27 vs. 280.07 ± 9.85 , 217.85 ± 7.47 vs. 302.98 ± 11.49 , 218.85 ± 14.51 vs. 359.74 ± 16.54 ; $p < 0.05-0.001$), suggesting the participation of the cAMP/CREB pathway following H3R signaling in the reduction of A β -mediated deficits by LC1405 using copper to trigger neurotoxicity of A β .

Histamine H3 receptor is related to PI3K/AKT/GSK3 β cascade that play a role in neuronal survival, thereby exerting neuroprotection on lesions due to multiple cytotoxic factors (Provensi et al., 2016). Copper-triggered A β exposure



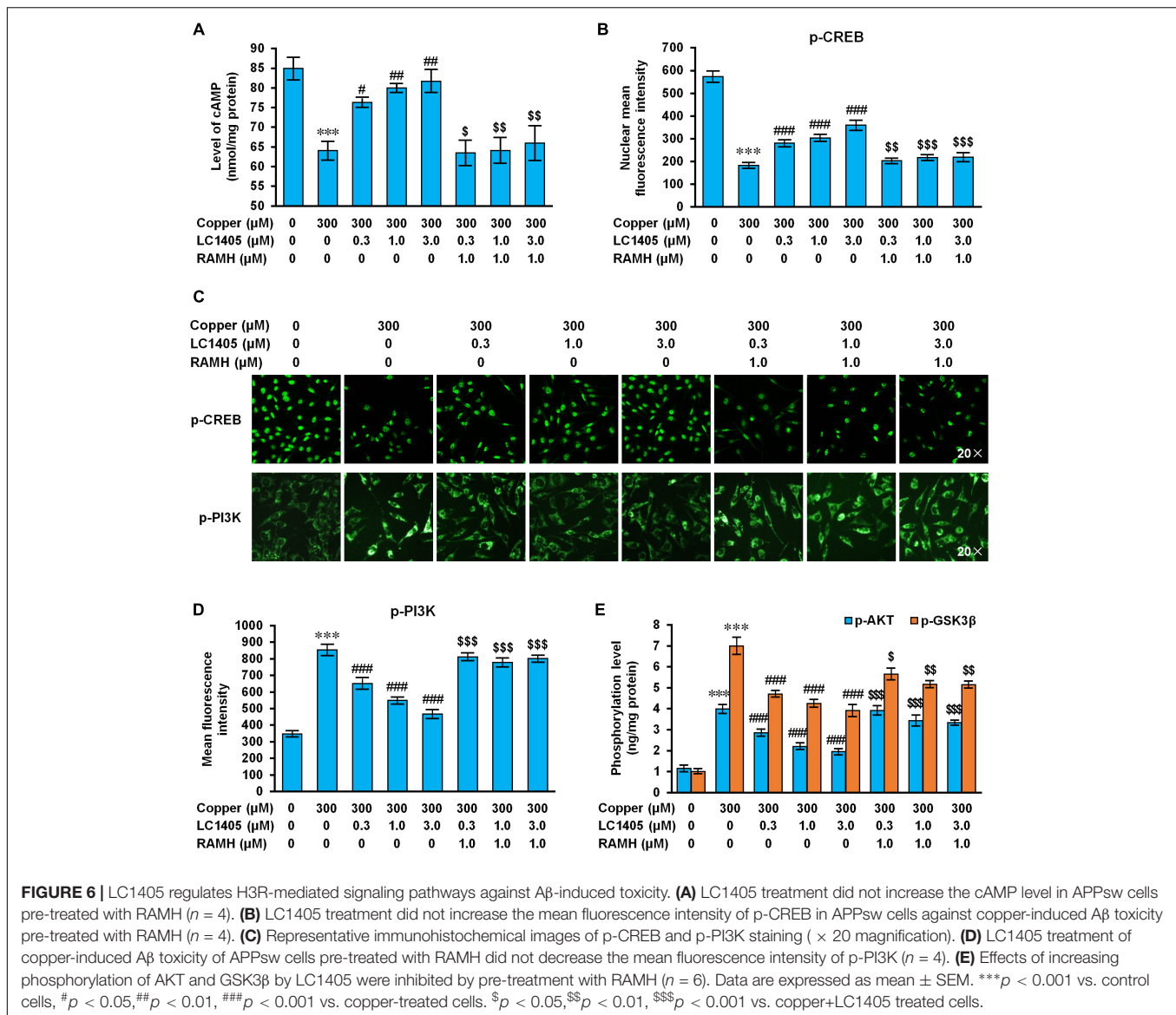
increased the phosphorylated level of PI3K, AKT, and GSK3 β (Figures 6C–E) (p-PI3K: 853.62 ± 26.34 vs. 347.84 ± 10.75 ; p-AKT: 3.98 ± 0.16 ng/mg protein vs. 1.23 ± 0.11 ng/mg protein; p-GSK3 β : 7.00 ± 0.36 ng/mg protein vs. 1.00 ± 0.07 ng/mg protein; all $p < 0.001$), whereas LC1405 treatment at the concentration of 0.3 μ M, 1.0 μ M, and 3.0 μ M prevented the increased phosphorylation of PI3K, AKT, and GSK3 β in APPsw cells after exposure to copper (p-PI3K: 651.74 ± 26.29 , 548.64 ± 12.29 , 467.27 ± 18.17 vs. 853.62 ± 26.34 ; p-AKT: 2.85 ± 0.12 ng/mg protein, 2.20 ± 0.10 ng/mg protein, 1.94 ± 0.08 ng/mg protein vs. 3.98 ± 0.16 ng/mg protein; p-GSK3 β : 4.70 ± 0.11 ng/mg protein, 4.25 ± 0.13 ng/mg protein, 3.90 ± 0.23 ng/mg protein vs. 7.00 ± 0.36 ng/mg protein; all $p < 0.001$). However, in response to RAMH, H3R activation affected the LC1405 effect of preventing the increased phosphorylation of PI3K, AKT, and GSK3 β induced by copper (p-PI3K: 810.88 ± 16.18 vs. 651.74 ± 26.29 , 778.13 ± 19.69 vs. 548.64 ± 12.29 , 801.26 ± 13.68 vs. 467.27 ± 18.17 ; p-AKT: 3.92 ± 0.15 ng/mg protein vs. 2.85 ± 0.12 ng/mg protein, 3.42 ± 0.21 ng/mg protein vs. 2.20 ± 0.10 ng/mg protein, 3.33 ± 0.06 ng/mg protein vs. 1.94 ± 0.08 ng/mg protein; p-GSK3 β : 5.66 ± 0.22 ng/mg protein vs. 4.70 ± 0.11 ng/mg protein, 5.17 ± 0.11 ng/mg protein vs. 4.25 ± 0.13 ng/mg protein, 5.15 ± 0.12 ng/mg protein vs. 3.90 ± 0.23 ng/mg protein; $p < 0.05$ – 0.001). These observations indicated that H3R-mediated PI3K/AKT/GSK3 β signaling is involved in the protective role of LC1405 against copper-induced A β cytotoxicity.

Based on the observations above, LC1405 protected neurons against copper-triggered A β -induced toxicity through H3R-dependent cAMP/CREB and PI3K/AKT/GSK3 β signaling.

DISCUSSION

Two major contributions are provided by this study to elucidate the underlying mechanism of action of LC1405. First, LC1405 was identified as a prospective H3R antagonist that prevented A β -induced neurotoxicity and as a potential treatment of AD both *in vitro* and *in vivo*. Second, a cellular signaling profile of LC1405 in H3R antagonism was provided, characterized by a beneficial H3R-dependent signaling of cAMP/CREB and AKT/GSK3 β axes. These findings revealed novel evidence and insights that focus on the role of H3R, which might be a potential therapeutic target in the treatment of AD.

From a previous multi-step screening process, LC1405 was identified as a potential H3R-targeting compound as a result of *in silico* prediction of H3R ligands, and subsequent cell-based-target assays on H3Rs and *in vitro* neuroprotective evaluation (see **Supplementary Material**). Furthermore, the ability of LC1405 in reversing the effects of AD and underlying mechanisms were evaluated in APP/PS1 double transgenic mice, and SH-SY5Y cells that express APP with a familial Swedish mutation, both excessively expressing the APP gene



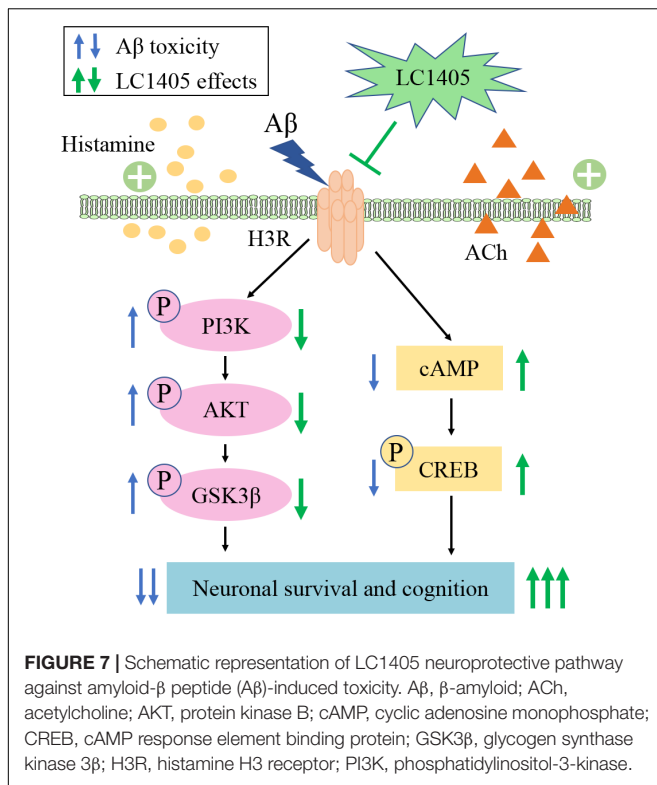
and mimicking β -amyloidogenic disturbance (Zhang et al., 2006; Voss et al., 2014).

Our study found that LC1405 improved learning and memory deficits in AD mice (Figures 1B–G). Consistent with these findings, neurodegeneration and ultrastructural abnormalities were rescued in the hippocampal and cortical regions (Figures 2A–C). Importantly, these alterations were in line with the *in vitro* cytoprotection and apoptotic preservation demonstrated after LC1405 treatment (Figures 4A–D). Thus, treatment with LC1405 is a promising approach in ameliorating the pathology of AD.

Excessive oxidation has been recognized as a contributor to A β -induced neurotoxicity with metal dyshomeostasis being implicated in the A β aggregation process of AD. Extremely high ion concentrations, such as copper, have been found colocalized with A β deposits in the AD-affected brain (Jakob-Roetne and Jacobsen, 2009; Duce and Bush, 2010). In addition,

redox active copper ions lead to ROS overproduction, resulting in oxidative damage that triggers neurodegeneration of the brain (Huang et al., 1999; Jakob-Roetne and Jacobsen, 2009). Here, limited antioxidative effects were obtained after LC1405 treatment in APP/PS1 mice, as indicated by the limited reduction in oxidative biomarkers, such as MDA, SOD, and GSH-Px (Figures 2G–I). Thus, LC1405 did not provide a sufficient antioxidant effect through scavenging ROS generation due to A β -mediated neurotoxicity related with AD.

The widely accepted amyloid hypothesis suggests that the assembly of A β to form aggregates, involving oligomers, protofibrils, fibrils, and even senile plaques, is a central event in the progression of AD (Ferreira et al., 2015; Gulisano et al., 2018). Various reports also confirmed that aggregated A β are toxic to neuronal cells, thereby indicating that inhibition of A β aggregation as a potential AD therapy is a reasonable strategy in AD treatment. However, the results



from pathological, biological, and western blotting experiments showed that LC1405 treatment did not provide a significant reduction in A β burden in APP/PS1 mice (**Figures 2C–F**), which resulted in A β plaque deposition as early as 2 months of age and moderate levels of A β deposition at the age of 5 months (Blanchard et al., 2003; Ding et al., 2008).

Apart from A β aggregation and deposition, the β -amyloidogenic pathway in which A β is produced through APP cleavage by BACE1 also plays a role in the evaluation of neuroprotective agents. LC1405 was found to possess a weak inactivation effect on BACE-1 (**Figure 4G**). This result partly explained the limited down-regulation of APP expression *in vitro* and failure of lowering multiple forms of A β levels, including soluble and insoluble A β , A11-immunoreactive prefibrillar oligomers, and amyloid aggregates/misfolded proteins or similar (**Figures 2D–F, 4C,E,F**). Therefore, we initially presumed that the beneficial effect of LC1405 on enhancing learning capacity and reducing memory deficits might be independent of changes in the amyloidogenic processing of APP, or in the process of secretion or deposition of A β . Although we found that LC1405 was effective in rescuing neuronal cell viability due to fibrillar A $\beta_{1-40/42}$ toxicity (**Supplementary Figure 2**), whether LC1405 had the definite effect on altering aggregation profile of A β should be further studied on the synthetic peptide and Alzheimer-related animal models.

In the part of the brain that is responsible for learning and memory, H3R, both for integrity and function, is conserved in A β over-expressing regions (Foley et al., 2009), indicating that H3R may neither participate in the amyloidogenic processing of

APP nor alter the secretion or deposition of A β . In our study, LC1405 might preferentially produce improvements in cognition and neuroprotective effects by altering H3R-dependent processes rather than by reducing A β deposition or decreasing oxidative stress. Two potential beneficial effects of LC1405 involved in preventing A β toxicity were identified in this work: LC1405 (i) improved cholinergic activity by up-regulating ACh and histamine release; (ii) maintained cognitive molecular cascades of H3R-dependent transduction, involving cAMP/CREB and AKT/GSK3 β signaling pathways.

Histamine H3 receptor is an auto- and heteroreceptor that negatively regulates the release of histamine and several cognition-related key neurotransmitters, such as ACh, which is recognized as a major neurochemical modulator of cognitive processing, particularly in AD (Bartus, 2000). In this study, we found that oral administration of LC1405 increased the levels of histamine and ACh in mouse brain (**Figures 3C,D**), which was in accordance with the hypothesis that H3R antagonists increased neurotransmitter levels involving ACh and histamine in the brain, thus counteracting AD deficits (Bitner et al., 2011). H3Rs on histaminergic neurons provide tonic inhibition of the firing rate (Jin and Panula, 2005), whereas those on presynaptic histaminergic terminals restrict histamine synthesis and release (Arrang et al., 1983, 1987). Therefore, our hypothesis was that LC1405 administration might inhibit presynaptic H3 autoreceptor activation and increase histamine levels in the synaptic cleft. In addition, long-term administration of LC1405 increased ACh levels in the brain without the influence of AChE activity (**Figures 3A,B**). Since an *in vivo* micro-dialysis assay suggested that hetero-H3R-mediated regulation of ACh is related to potassium levels in different regions of the brain (Blandina et al., 1996), but not by counteracting the activation of histamine H1 or the H2 subtype (Esbenshade et al., 2008), our conclusion was that in response to A β toxicity, LC1405 treatment might increase endogenous ACh synthesis or its release in cholinergic neurons that have been stimulated by increased histamine derived from over-activated histaminergic terminals through the antagonistic action of H3R, rather than by increasing synaptic ACh via a reduction in enzymatic degradation by AChE.

Activation of H3Rs mediates a series of intracellular signaling pathways that are involved in the pathogenesis of AD, including the G $\alpha_{i/o}$ -protein-coupled inhibition of AC (Lovenberg et al., 1999), downstream exaggeration of cognitive decline through transduction of cAMP/CREB (Moreno et al., 2011), and activation of PI3K/AKT/GSK3 β signaling (Rapanelli et al., 2016). Constitutively active H3R inhibits cAMP increase, which would otherwise activate PKA phosphorylation of CREB (Shi et al., 2012), an important signaling molecule located in the cell nucleus and responsible for the synaptic plasticity implicated in the cognitive function. In agreement with this hypothesis, in our study, cAMP/CREB signaling was seriously weakened in A β -mediated Alzheimer's pathogenesis, whereas LC1405 rescued aberrant cAMP/CREB signaling both *in vitro* and *in vivo* (**Figures 3E,F, 6A,B**). When APPsw cells that were pretreated with the H3R agonist (RAMH) were treated with LC1405 in the presence of copper, restoration of the cAMP/CREB signaling pathway was completely abolished (**Figures 6A,B**). Therefore,

these results suggested that H3R inactivation of LC1405 plays a pivotal role in neuronal transduction of the cAMP/CREB pathway in response to A β neurotoxicity. It is reasonable to believe that the ability of LC1405, as a H3R antagonist, to stimulate the release of histamine and ACh might lead to specific cellular signaling events as a property of auto-receptors in the phosphorylation-activation of CREB that contributed to enhanced cognitive function.

Besides H3R-mediated signaling through G $\alpha_{i/o}$ -proteins, G $\beta\gamma$ -subunits are known to activate specific signal transduction pathways involving the PI3K/AKT/GSK3 β cascade (Rapanelli et al., 2016). Similar to other G protein-coupled receptor (GPCR) signaling transduction, H3R activation results in AKT phosphorylation at Ser 473 and subsequently GSK3 β hyperphosphorylation occurring from increased phosphorylation of S9 through PI3K activation via the G $\beta\gamma$ -subunits of G $\alpha_{i/o}$ proteins, previously demonstrated in a neuroblastoma cell line, primary cultures of cortical neurons, and in striatal slices of Sprague-Dawley rats (Bongers et al., 2007). Several studies support the findings that H3R antagonists function as indirect inhibitors of GSK3 β , thereby resulting in decreased S9 phosphorylation and exert therapeutic effects in neurodegenerative disorders beyond amelioration of symptoms (Vohora and Bhowmik, 2012). Consistent with these studies, our results showed that the PI3K/AKT/GSK3 β pathway was one pathway involved in LC1405 neuroprotection, which could be diminished by a H3R agonist (Figures 3G,H, 6C–E). In this regard, H3R-mediated postsynaptic PI3K/AKT/GSK3 β cascade resulted involved in LC1405-induced neuroprotection against A β neurotoxicity.

Prior to the identification of the anti-AD effects of LC1405, the safe dosage of LC1405 was evaluated from 0.3 to 10.0 μ M *in vitro* and long-term oral administration at 3 mg/kg *in vivo* (Figures 2B–G, 4A). The phenomenon that LC1405 alone activated cAMP/CREB cascade was in accordance to the fact that LC1405 targets H3Rs with the specific GPCR characteristics (Figures 3E,F). Since PI3K/AKT/GSK3 β signaling pathway was regulated by several factors, we concluded that in a physiological state, a single factor mediated by LC1405 influencing PI3K/AKT/GSK3 β pathway resulted in well-balanced effects. Therefore, LC1405 could trigger PI3K/AKT/GSK3 β pathway and attenuate cognition deficits under physiological, but not pathological, conditions.

In summary, LC1405 had beneficial effects on blocking A β -induced neuronal stress both *in vitro* and *in vivo*. Anti-H3R therapy using LC1405 did not affect A β burden or fully alter the redox balance system, but was effective in increasing the level of histamine and ACh in the brain. LC1405 improved cognition through H3R-dependent cellular

signaling cascades involving cAMP/CREB and AKT/GSK3 β pathways (Figure 7). Taken together, our results demonstrated that LC1405 ameliorated cognitive deficits by blocking H3R-modulated signaling transduction against A β -induced cellular stress. Thus, LC1405 may be a prospective H3R antagonist that holds a potential in controlling disease progression in AD patients, who already developed cognitive deficits with H3R-related ACh neurotransmission abnormalities.

ETHICS STATEMENT

All of the protocols dealing with the maintenance and handling of animals were followed as stated in the Guidelines of the Institute of Medicinal Biotechnology, Chinese Academy of Medical Sciences.

AUTHOR CONTRIBUTIONS

LW performed the *in vivo* experiments. JE, HJ, QW, and SX performed the *in vitro* experiments. JF performed the *in silico* experiments. LW and JF employed statistical analysis and wrote the manuscript. RL and ZL performed principal investigation, and revised and edited the manuscript. All authors read and approved the final manuscript.

FUNDING

This study was supported by the National Natural Science Foundation of China (No. U1803281 and 81673411), the Non-profit Central Research Institute Fund of Chinese Academy of Medical Sciences (2018RC350013), and Chinese Academy of Medical Sciences (CAMS) Innovation Fund for Medical Science (2017-I2M-1-016).

ACKNOWLEDGMENTS

We thank Prof. Dong-mei Wang, Institute of Materia Medica, Chinese Academy of Medical Sciences and Peking Union Medical College, for providing all the active compounds.

SUPPLEMENTARY MATERIAL

The Supplementary Material for this article can be found online at: <https://www.frontiersin.org/articles/10.3389/fnins.2019.00334/full#supplementary-material>

REFERENCES

- Arrang, J. M., Garbarg, M., and Schwartz, J. C. (1983). Auto-inhibition of brain histamine-release mediated by a novel class (H3) of histamine-receptor. *Nature* 302, 832–837.
- Arrang, J. M., Garbarg, M., and Schwartz, J. C. (1987). Autoinhibition of histamine synthesis mediated by presynaptic H3 receptors. *Neuroscience* 23, 149–157.
- Bacciottini, L., Passani, M. B., Giovannelli, L., Cangioli, I., Mannaioni, P. F., Schunack, W., et al. (2002). Endogenous histamine in the medial septum-diagonal band complex increases the release of acetylcholine from the

- hippocampus: a dual-probe microdialysis study in the freely moving rat. *Eur. J. Neurosci.* 15, 1669–1680.
- Ballard, C., Gauthier, S., Corbett, A., Brayne, C., Aarsland, D., and Jones, E. (2011). Alzheimer's disease. *Lancet* 377, 1019–1031. doi: 10.1016/S0140-6736(10)61349-9
- Ballok, D. A., Millward, J. M., and Sakic, B. (2003). Neurodegeneration in autoimmune MRL-lpr mice as revealed by Fluoro Jade B staining. *Brain Res.* 964, 200–210.
- Bardgett, M. E., Davis, N. N., Schultheis, P. J., and Griffith, M. S. (2011). Ciproxifan, an H3 receptor antagonist, alleviates hyperactivity and cognitive deficits in the APP Tg2576 mouse model of Alzheimer's disease. *Neurobiol. Learn Mem.* 95, 64–72. doi: 10.1016/j.nlm.2010.10.008
- Bartus, R. T. (2000). On neurodegenerative diseases, models, and treatment strategies: lessons learned and lessons forgotten a generation following the cholinergic hypothesis. *Exp. Neurol.* 163, 495–529.
- Bhowmik, M., Saini, N., and Vohora, D. (2014). Histamine H3 receptor antagonism by ABT-239 attenuates kainic acid induced excitotoxicity in mice. *Brain Res.* 1581, 129–140. doi: 10.1016/j.brainres.2014.06.012
- Bitner, R. S., Markosyan, S., Nikkel, A. L., and Brioni, J. D. (2011). In-vivo histamine H3 receptor antagonism activates cellular signaling suggestive of symptomatic and disease modifying efficacy in Alzheimer's disease. *Neuropharmacology* 60, 460–466. doi: 10.1016/j.neuropharm.2010.10.026
- Blanchard, V., Moussaoui, S., Czech, C., Touchet, N., Bonici, B., Planche, M., et al. (2003). Time sequence of maturation of dystrophic neurites associated with Abeta deposits in APP/PS1 transgenic mice. *Exp. Neurol.* 184, 247–263.
- Blandina, P., Giorgetti, M., Bartolini, L., Cecchi, M., Timmerman, H., Leurs, R., et al. (1996). Inhibition of cortical acetylcholine release and cognitive performance by histamine H3 receptor activation in rats. *Br. J. Pharmacol.* 119, 1656–1664.
- Bonaventure, P., Letavic, M., Dugovic, C., Wilson, S., Aluisio, L., Pudiak, C., et al. (2007). Histamine H3 receptor antagonists: from target identification to drug leads. *Biochem. Pharmacol.* 73, 1084–1096. doi: 10.1016/j.bcp.2006.10.031
- Bongers, G., Bakker, R. A., and Leurs, R. (2007). Molecular aspects of the histamine H3 receptor. *Biochem. Pharmacol.* 73, 1195–1204. doi: 10.1016/j.bcp.2007.01.008
- Browman, K. E., Komater, V. A., Curzon, P., Rueter, L. E., Hancock, A. A., Decker, M. W., et al. (2004). Enhancement of prepulse inhibition of startle in mice by the H3 receptor antagonists thioperamide and ciproxifan. *Behav. Brain Res.* 153, 69–76. doi: 10.1016/j.bbr.2003.11.001
- Brown, J. W., Whitehead, C. A., Basso, A. M., Rueter, L. E., and Zhang, M. (2013). Preclinical evaluation of non-imidazole histamine H3 receptor antagonists in comparison to atypical antipsychotics for the treatment of cognitive deficits associated with schizophrenia. *Int. J. Neuropsychopharmacol.* 16, 889–904. doi: 10.1017/S1461145712000739
- Carvajal, F. J., Zolezzi, J. M., Tapia-Rojas, C., Godoy, J. A., and Inestrosa, N. C. (2013). Tetrahydroperforin decreases cholinergic markers associated with amyloid-beta plaques, 4-hydroxynonenal formation, and caspase-3 activation in A β PP/PS1 mice. *J. Alzheimers Dis.* 36, 99–118. doi: 10.3233/JAD-130230
- Chiang, K., and Koo, E. H. (2014). Emerging therapeutics for Alzheimer's disease. *Annu. Rev. Pharmacol. Toxicol.* 54, 381–405.
- Clapham, J., and Kilpatrick, G. J. (1992). Histamine H3 receptors modulate the release of [3H]-acetylcholine from rat entorhinal cortex—evidence for the possible existence of H3 receptor subtypes. *Br. J. Pharmacol.* 107, 919–923.
- Ding, Y., Qiao, A., Wang, Z., Goodwin, J. S., Lee, E. S., Block, M. L., et al. (2008). Retinoic acid attenuates beta-amyloid deposition and rescues memory deficits in an Alzheimer's disease transgenic mouse model. *J. Neurosci.* 28, 11622–11634. doi: 10.1523/JNEUROSCI.3153-08.2008
- Duce, J. A., and Bush, A. I. (2010). Biological metals and Alzheimer's disease: implications for therapeutics and diagnostics. *Prog. Neurobiol.* 92, 1–18. doi: 10.1016/j.pneurobio.2010.04.003
- Dumas, J. A., and Newhouse, P. A. (2011). The cholinergic hypothesis of cognitive aging revisited again: cholinergic functional compensation. *Pharmacol. Biochem. Behav.* 99, 254–261. doi: 10.3233/JAD-130230
- Esbenshade, T. A., Browman, K. E., Bitner, R. S., Strakhova, M., Cowart, M. D., and Brioni, J. D. (2008). The histamine H3 receptor: an attractive target for the treatment of cognitive disorders. *Br. J. Pharmacol.* 154, 1166–1181. doi: 10.1038/bjp.2008.147
- Esbenshade, T. A., Fox, G. B., and Cowart, M. D. (2006). Histamine H3 receptor antagonists: preclinical promise for treating obesity and cognitive disorders. *Mol. Interv.* 59, 77–88.
- Ferreira, S. T., Lourenco, M. V., Oliveira, M. M., and De Felice, F. G. (2015). Soluble amyloid-beta oligomers as synaptotoxins leading to cognitive impairment in Alzheimer's disease. *Front. Cell Neurosci.* 9:191. doi: 10.3389/fncel.2015.00191
- Foley, A. G., Prendergast, A., Barry, C., Scully, D., Upton, N., Medhurst, A. D., et al. (2009). H3 receptor antagonism enhances NCAM PSA-mediated plasticity and improves memory consolidation in odor discrimination and delayed match-to-position paradigms. *Neuropsychopharmacology* 34, 2585–2600. doi: 10.1038/npp.2009.89
- Glabe, C. G. (2008). Structural classification of toxic amyloid oligomers. *J. Biol. Chem.* 283, 29639–29643. doi: 10.1074/jbc.R800016200
- Gulisano, W., Melone, M., Li Puma, D. D., Tropea, M. R., Palmeri, A., Arancio, O., et al. (2018). The effect of amyloid- β peptide on synaptic plasticity and memory is influenced by different isoforms, concentrations, and aggregation status. *Neurobiol. Aging* 71, 51–60. doi: 10.1016/j.neurobiolaging.2018.06.025
- Huang, X., Atwood, C. S., Hartshorn, M. A., Multhaup, G., Goldstein, L. E., Scarpa, R. C., et al. (1999). The A beta peptide of Alzheimer's disease directly produces hydrogen peroxide through metal ion reduction. *Biochemistry* 38, 7609–7616. doi: 10.1021/bi990438f
- Jakob-Roetne, R., and Jacobsen, H. (2009). Alzheimer's disease: from pathology to therapeutic approaches. *Angew. Chem. Int. Ed. Engl.* 48, 3030–3059. doi: 10.1002/anie.200802808
- Jin, C. Y., and Panula, P. (2005). The laminar histamine receptor system in human prefrontal cortex suggests multiple levels of histaminergic regulation. *Neuroscience* 132, 137–149. doi: 10.1016/j.neuroscience.2004.12.017
- Ligneau, X., Lin, J., Vanni-Mercier, G., Jouvet, M., Muir, J. L., Ganellin, C. R., et al. (1998). Neurochemical and behavioral effects of ciproxifan, a potent histamine H3-receptor antagonist. *J. Pharmacol. Exp. Ther.* 287, 658–666.
- Liu, Q. S., Jiang, H. L., Wang, Y., Wang, L. L., Zhang, J. X., He, C. H., et al. (2018). Total flavonoid extract from *Dracocephalum moldavica* L. attenuates β -amyloid-induced toxicity through anti-amyloidogenic and neurotrophic pathways. *Life Sci.* 193, 214–225. doi: 10.1016/j.lfs.2017.10.041
- Liu, R., Li, J. Z., Song, J. K., Zhou, D., Huang, C., Bai, X. Y., et al. (2014). Pinocembrin improves cognition and protects the neurovascular unit in Alzheimer-related deficits. *Neurobiol. Aging* 35, 1275–1285. doi: 10.1016/j.neurobiolaging.2013.12.031
- Liu, R., Wu, C. X., Zhou, D., Yang, F., Tian, S., Zhang, L., et al. (2012). Pinocembrin protects against β -amyloid-induced toxicity in neurons through inhibiting receptor for advanced glycation end products (RAGE)-independent signaling pathways and regulating mitochondrion-mediated apoptosis. *BMC Med.* 10:105. doi: 10.1186/1741-7015-10-105
- Lovenberg, T. W., Roland, B. L., Wilson, S. J., Jiang, X., Pyati, J., Huvar, A., et al. (1999). Cloning and functional expression of the human histamine H3 receptor. *Mol. Pharmacol.* 55, 1101–1107.
- Mani, V., Jaafar, S. M., Azahan, N. S. M., Ramasamy, K., Lim, S. M., Ming, L. C., et al. (2017). Ciproxifan improves cholinergic transmission, attenuates neuroinflammation and oxidative stress but does not reduce amyloid level in transgenic mice. *Life Sci.* 180, 23–35. doi: 10.1016/j.lfs.2017.05.013
- Medhurst, A. D., Atkins, A. R., Beresford, I. J., Brackenborough, K., Briggs, M. A., Calver, A. R., et al. (2007). GSK189254, a novel H3 receptor antagonist that binds to histamine H3 receptors in Alzheimer's disease brain and improves cognitive performance in preclinical models. *J. Pharmacol. Exp. Ther.* 321, 1032–1045. doi: 10.1124/jpet.107.120311
- Moreno, E., Hoffmann, H., Gonzalez-Sepúlveda, M., Navarro, G., Casadó, V., Cortés, A., et al. (2011). Dopamine D1-histamine H3 receptor heteromers provide a selective link to MAPK signaling in GABAergic neurons of the direct striatal pathway. *J. Biol. Chem.* 286, 5846–5854. doi: 10.1074/jbc.M110.161489
- Nasehi, M., Sharifi, S., and Zarrindast, M. R. (2012). Involvement of the cholinergic system of CA1 on harmaline-induced amnesia in the step-down passive avoidance test. *J. Psychopharmacol.* 26, 1151–1161. doi: 10.1177/0269881111421972
- Provensi, G., Costa, A., Passani, M. B., and Blandina, P. (2016). Donepezil, an acetylcholine esterase inhibitor, and ABT-239, a histamine H3 receptor antagonist/inverse agonist, require the integrity of brain histamine system to exert biochemical and procognitive effects in the mouse. *Neuropharmacology* 109, 139–147. doi: 10.1016/j.neuropharm.2016.06.010

- Rapanelli, M., Frick, L. R., Horn, K. D., Schwarcz, R. C., Pogorelov, V., Nairn, A. C., et al. (2016). The histamine H3 receptor differentially modulates Mitogen-Activated Protein Kinase (MAPK) and Akt signaling in striatonigral and striatopallidal neurons. *J. Biol. Chem.* 291, 21042–21052. doi: 10.1074/jbc.M116.731406
- Shi, Y., Sheng, R., Zhong, T., Xu, Y., Chen, X., Yang, D., et al. (2012). Identification and characterization of ZEL-H16 as a novel agonist of the histamine H3 receptor. *PLoS. One* 7:e42185. doi: 10.1371/journal.pone.0042185
- Vohora, D., and Bhowmik, M. (2012). Histamine H3 receptor antagonists/inverse agonists on cognitive and motor processes: relevance to Alzheimer's disease, ADHD, schizophrenia, and drug abuse. *Front. Syst. Neurosci.* 6:72. doi: 10.3389/fnsys.2012.00072
- Vorhees, C. V., and Williams, M. T. (2006). Morris water maze: procedures for assessing spatial and related forms of learning and memory. *Nat. Protoc.* 1, 848–858. doi: 10.1038/nprot.2006.116
- Voss, K., Harris, C., Ralle, M., Duffy, M., Murchison, C., and Quinn, J. F. (2014). Modulation of tau phosphorylation by environmental copper. *Transl. Neurodegener.* 3:24. doi: 10.1186/2047-9158-3-24
- Yu, S. Q., Wang, J. S., Chen, S. Y., Liu, X. M., Li, Y., Ding, Y. M., et al. (2015). Diagnostic significance of intraoperative ultrasound contrast in evaluating the resection degree of brain glioma by transmission electron microscopic examination. *Chin. Med. J.* 128, 186–190. doi: 10.4103/0366-6999.149194
- Zhang, J., Mori, A., Chen, Q., and Zhao, B. (2006). Fermented papaya preparation attenuates beta-amyloid precursor protein: beta-amyloid-mediated copper neurotoxicity in beta-amyloid precursor protein and beta-amyloid precursor protein Swedish mutation overexpressing SH-SY5Y cells. *Neuroscience* 143, 63–72. doi: 10.1016/j.neuroscience.2006.07.023
- Zhao, L., Wang, J. L., Wang, Y. R., and Fa, X. Z. (2013). Apigenin attenuates copper-mediated beta-amyloid neurotoxicity through antioxidation, mitochondrion protection and MAPK signal inactivation in an AD cell model. *Brain Res.* 1492, 33–45. doi: 10.1016/j.brainres.2012.11.019

Conflict of Interest Statement: The authors declare that the research was conducted in the absence of any commercial or financial relationships that could be construed as a potential conflict of interest.

Copyright © 2019 Wang, Fang, Jiang, Wang, Xue, Li and Liu. This is an open-access article distributed under the terms of the Creative Commons Attribution License (CC BY). The use, distribution or reproduction in other forums is permitted, provided the original author(s) and the copyright owner(s) are credited and that the original publication in this journal is cited, in accordance with accepted academic practice. No use, distribution or reproduction is permitted which does not comply with these terms.